Strong redshift evolution in cluster RLF?

arXiv: 1103.3263 (in press)

Astronomy & Astrophysics manuscript no. lf.6.0
March 10, 2011

Redshift evolution of the 1.4 GHz volume averaged radio luminosity function in clusters of galaxies

M. W. Sommer[1,*], K. Basu[1,2], F. Pacaud[1], F. Bertoldi[1], and H. Andernach[3,1]

[1] Argelander-Institut für Astronomie, Auf dem Hügel 71,D-53121 Bonn, Germany
[2] Max Planck-Institut für Radioastronomie, Auf dem Hügel 69, D-53121 Bonn, Germany
[3] Permanent address: Departamento de Astronomía, Universidad de Guanajuato, AP 144, Guanajuato CP 36000, Mexico

Received ...; accepted ...

ABSTRACT

By cross-correlating large samples of galaxy clusters with publicly available radio source catalogs, we construct the volume-averaged radio luminosity function (RLF) in clusters of galaxies, and investigate its dependence on cluster redshift and mass. In addition, we determine the correlation between the cluster mass and the radio luminosity of the brightest source within 50 kpc from the cluster center. We use two cluster samples: the optically selected maxBCG cluster catalog and a composite sample of X-ray selected clusters. The radio data come from the VLA NVSS and FIRST surveys. We use scaling relations to estimate cluster masses and radii to get robust estimates of cluster volumes. We determine the projected radial distribution of sources, for which we find no dependence on luminosity or cluster mass. Background and foreground sources are statistically accounted for, and we account for confusion of radio sources by adaptively degrading the resolution of the radio source surveys. We determine the redshift evolution of the RLF under the assumption that its overall shape does not change with redshift. Our results are consistent with a pure luminosity evolution of the RLF in the range $0.1 \leq z \leq 0.3$ from the optical cluster sample. The X-ray sample extends to higher redshift and yields results also consistent with a pure luminosity evolution. We find no direct evidence of a dependence of the RLF on cluster mass from the present data, although the data are consistent with the most luminous sources only being found in high-mass systems.

Key words. Galaxies: clusters: general – Radio continuum: galaxies – Galaxies: active – Galaxies: evolution

Cluster sample

Main sample	maxBCG	X-ray	
clusters in main sample	13823	1177	
clusters with sufficient separation	12846	1121	
Sub-sample		**high-z**	**low-z**
Redshift range	$0.1 \leq z \leq 0.3$	$0.1 \leq z \leq 1.26$	$0.05 < z < 0.12$
Clusters within redshift range	12846	690	292
Clusters with $M > 5 \times 10^{13} M_\odot$	12522	674	275
clusters with NVSS coverage[a]	12475	596	218
clusters with FIRST coverage[a]	11812	273	75

Catalog	Number of clusters	Limiting flux (erg s^{-1} cm^{-2})
REFLEX	447	2.1e-12
NORAS	371	1.2e-12
160deg2	221	8.0e-14
400deg2	242	1.4e-13
WARPS1+2	124	8.0e-14
MACS(z>0.5)	12	7.0e-13

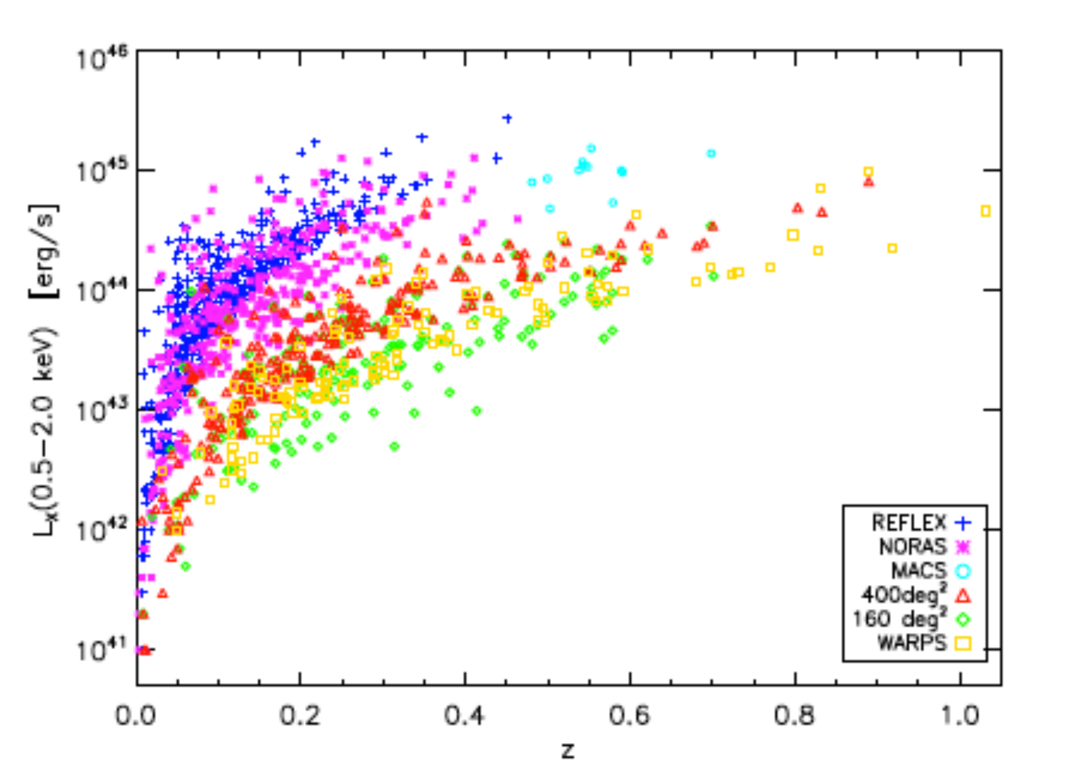

Radio luminosity of the BCGs

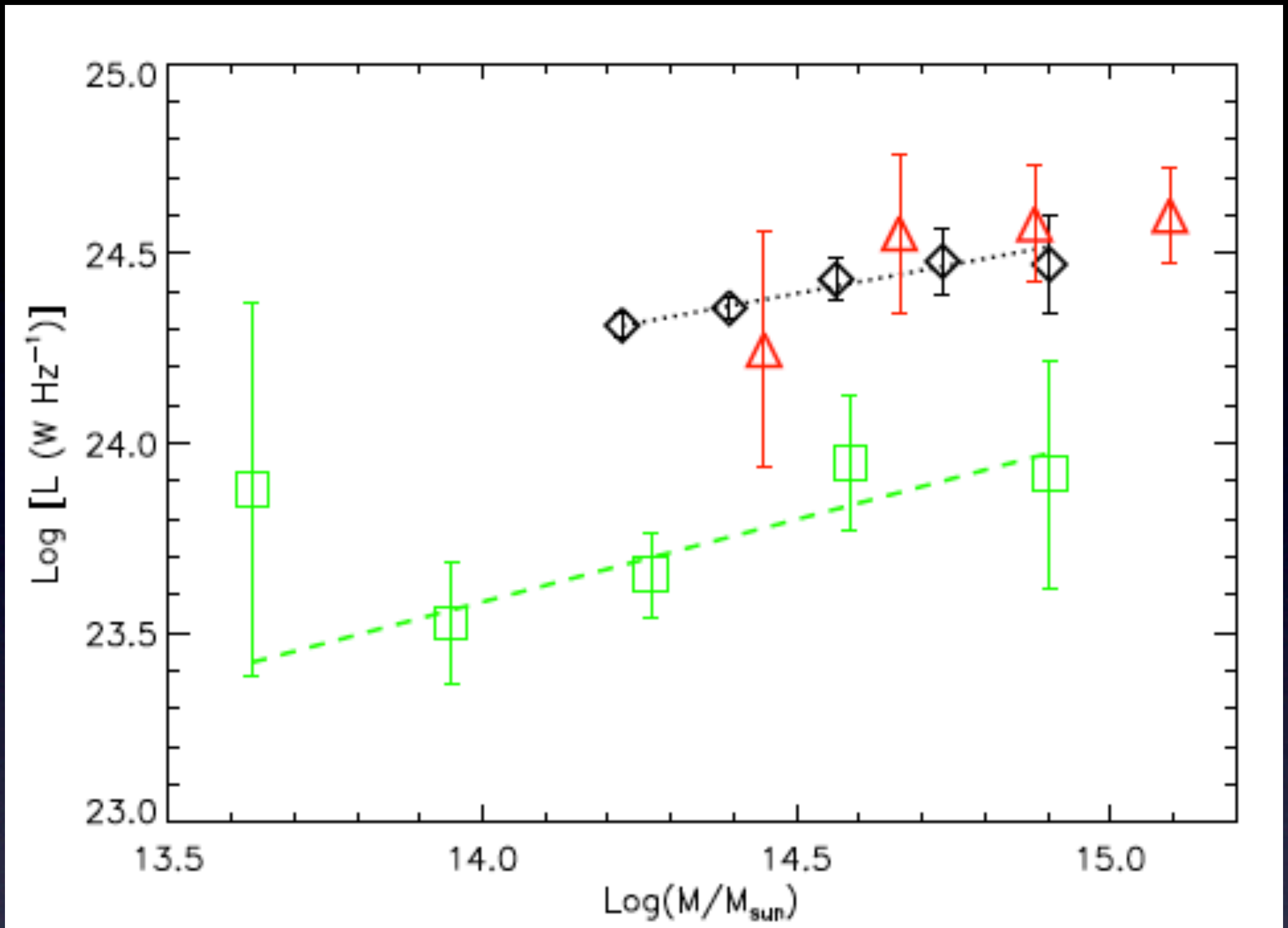

- Luminosity of the brightest source inside 50 kpc from center

- Similar weak correlation found by Lin & Mohr (2004), Croft et al. (2007), Haarsma et al. (2010) and others

- Deciphering redshift evolution is problematic because clusters can have multiple BCG or other non-BCG radio sources. Also there is a large scatter in the BCG radio luminosity.

Computing the luminosity function

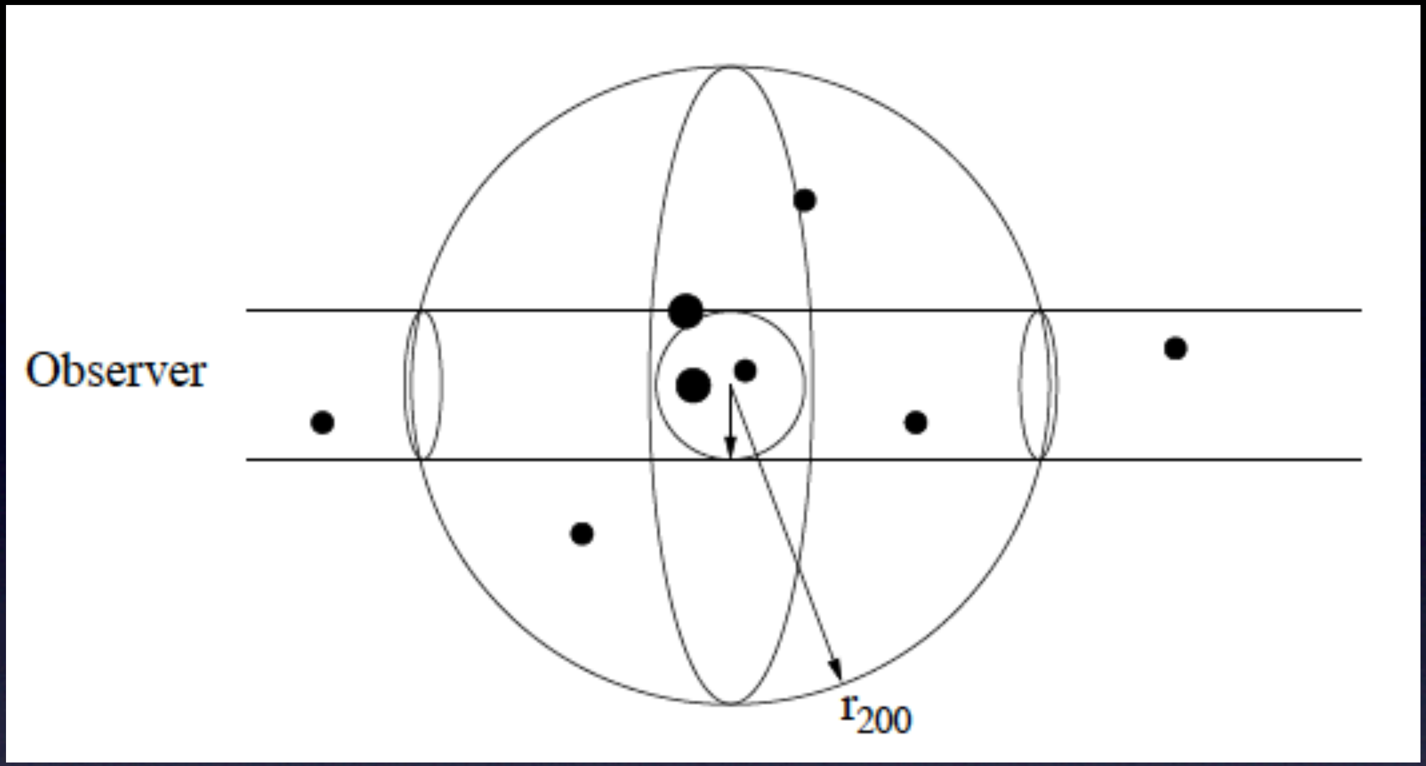

- Using a radial distribution, sources are de-projected in a sphere of radius r_{200}
- Source confusion is taken into account by artificially degrading the resolution (in radio catalogs) at lower redshift
- Effect of complex source morphology is checked by eye (to some extent!)

Radial source distribution

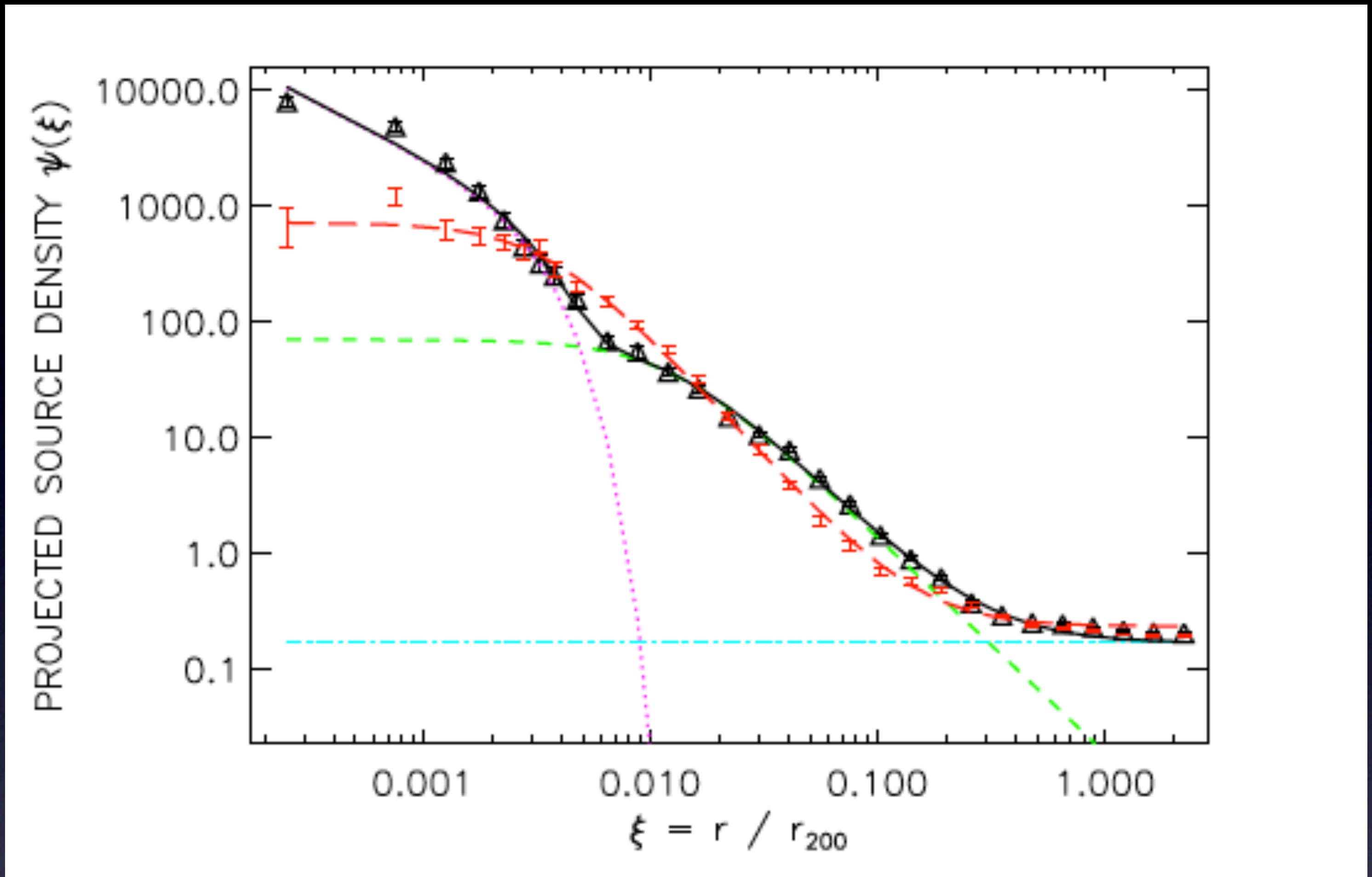

➡ Inner component modeled by a Gaussian, resulting from extended radio morphology of the BCG

➡ Outer component fitted with a β-model, corresponding to the distribution of radio sources

➡ The flat component is the field population

Radial source distribution

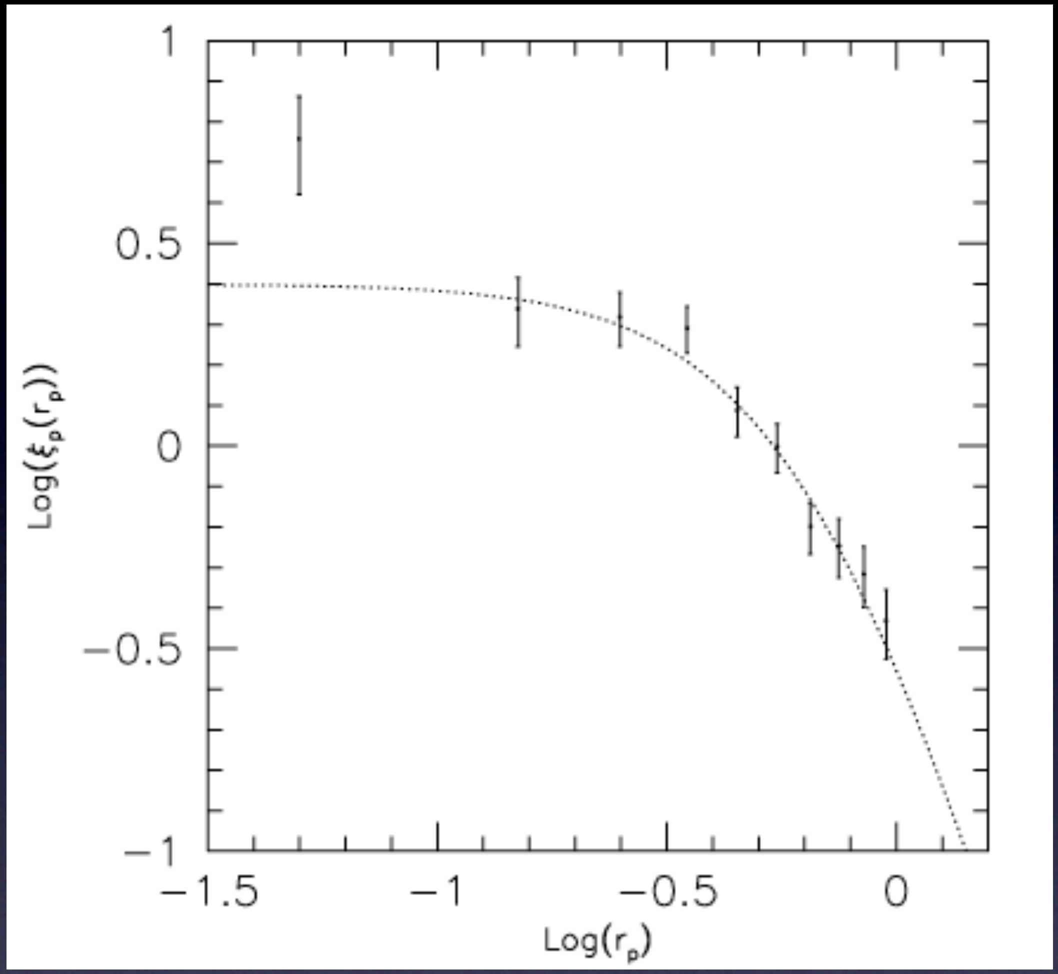

Massardi & De Zotti (2004)

951 Abell clusters + FIRST

(but fixed 1.5 Mpc radius!)

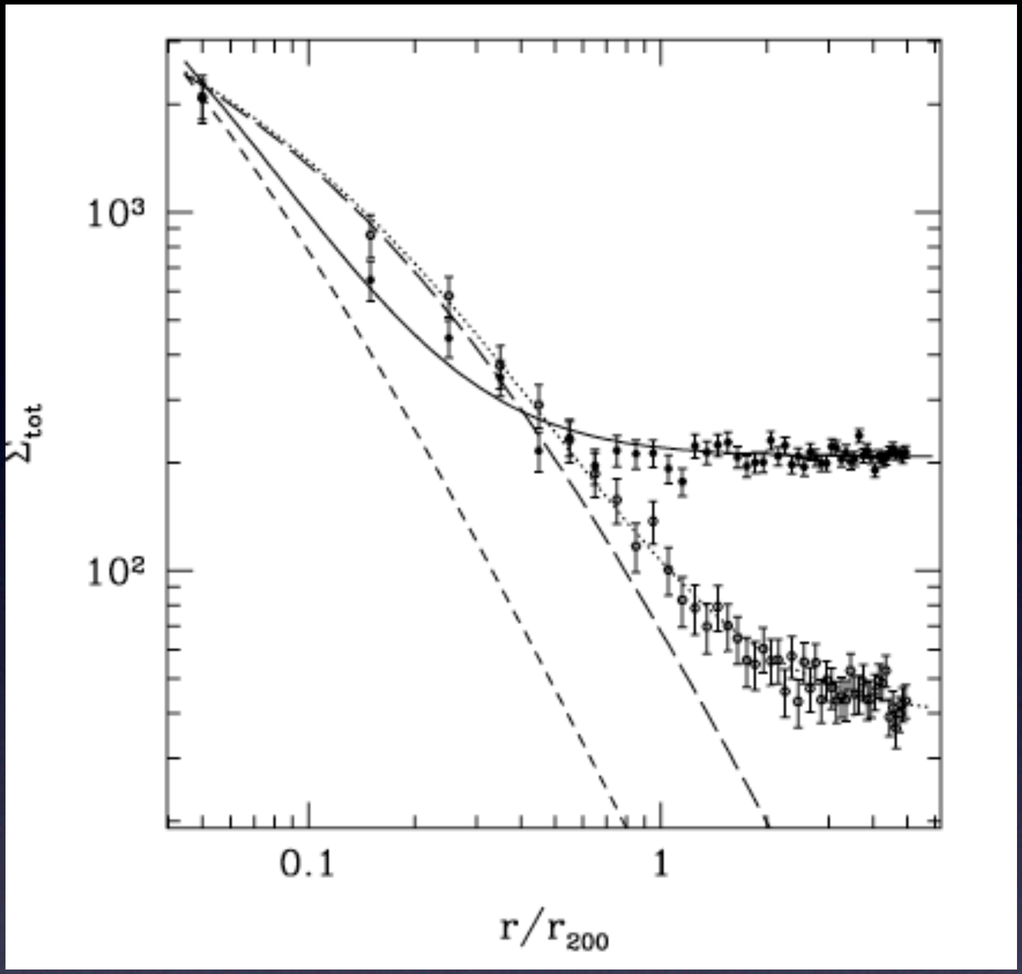

Lin & Mohr (2007)

573 X-ray clusters + NVSS

(also checked with 242
FIRST & NVSS clusters)

Radio luminosity function

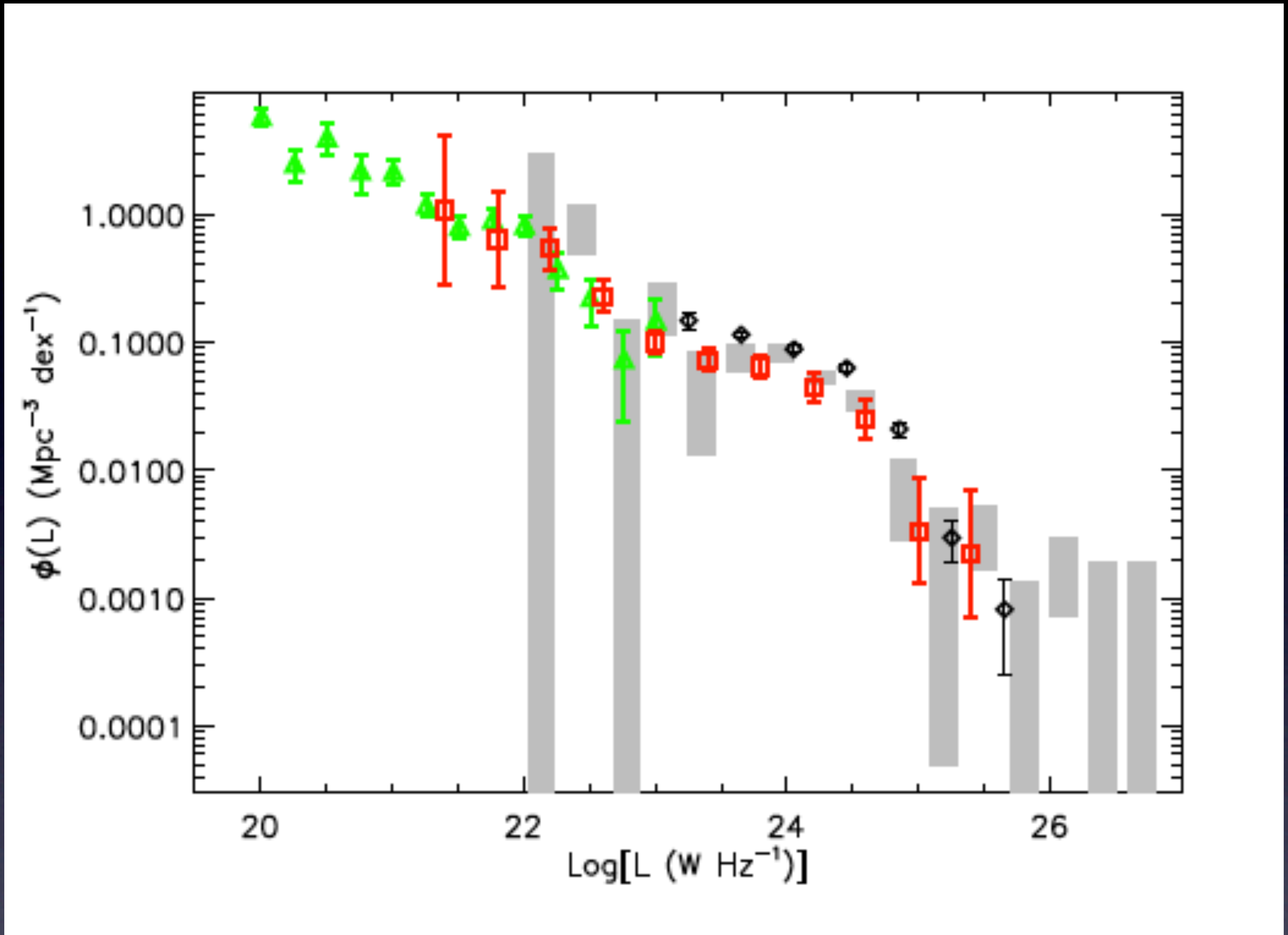

Result from a low-redshift (0.1 < z < 0.17) maxBCG sub-sample is compared with Lin & Mohr (2007) Massardi & De Zotti (2004) and Reddy & Yun (2004).

Modeling *z* and *M* dependence

Fit the luminosity function (Condon et al (2002, ..), Lin and Mohr (2007))

$$\log\phi = y - \left(b^2 + \left(\frac{\log L - x}{w}\right)^2\right)^{1/2} - 1.5\log L.$$

Under the assumption that the shape of the luminosity function does not vary with redshift, we can then write

$$\phi(L,z) \;=\; g(z)\,\phi\,[Lf(z), z\approx 0]\,,$$

and

$$L = L_0\left(\frac{1+z}{1+z_0}\right)^{\alpha_L},$$

$$\phi = \phi_0\left(\frac{1+z}{1+z_0}\right)^{\alpha_\phi},$$

Similarly for mass dependence

$$L \sim (M_{200})^{\gamma_L};$$
$$\phi \sim (M_{200})^{\gamma_\phi}.$$

Mass dependence

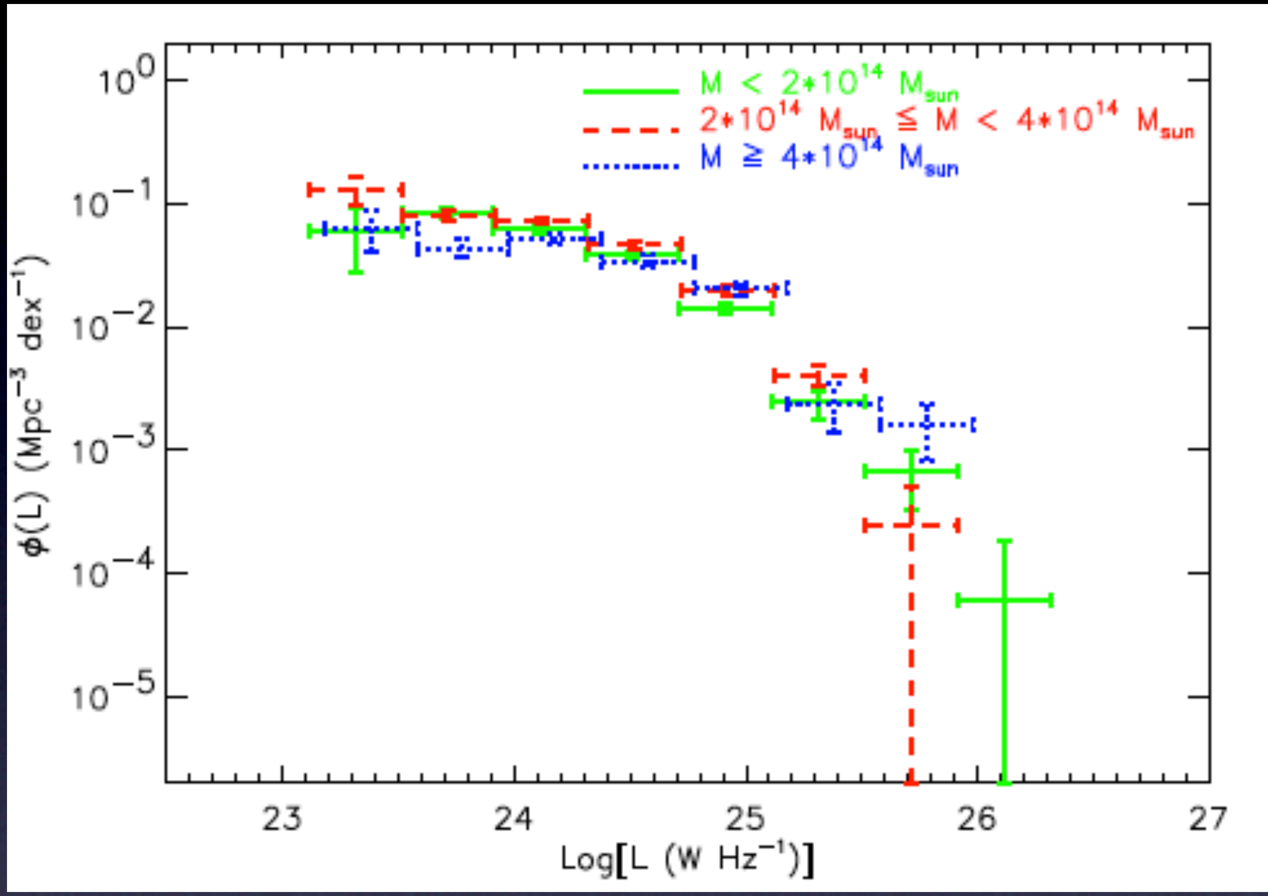

optical sample

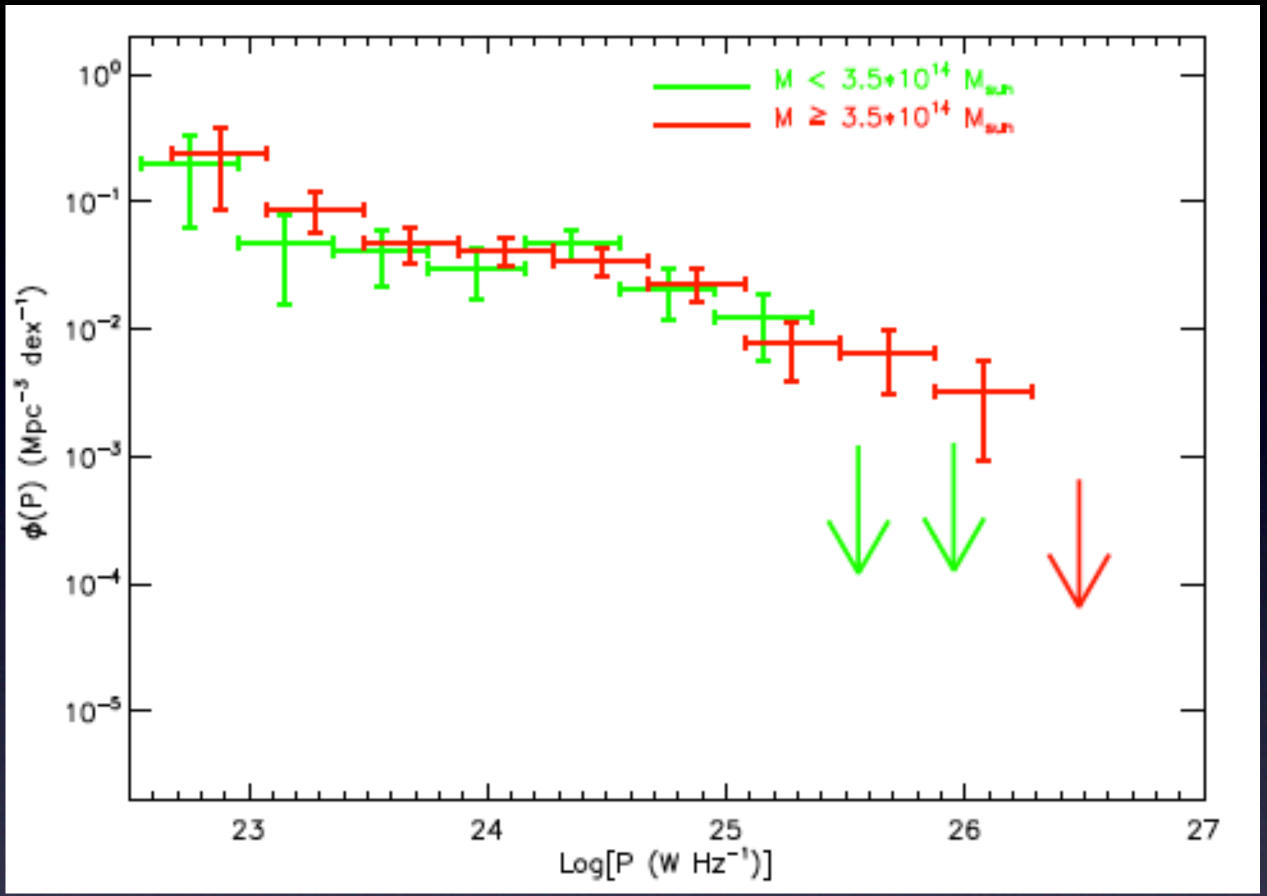

X-ray sample

✦ No conclusive evidence of mass dependence in the radio LF (although consistent with more luminous sources to be in more massive clusters)

✦ The mass effect possibly got offset by having more low-mass systems (smaller volume) and having no starburst population

Redshift evolution

Optical sample

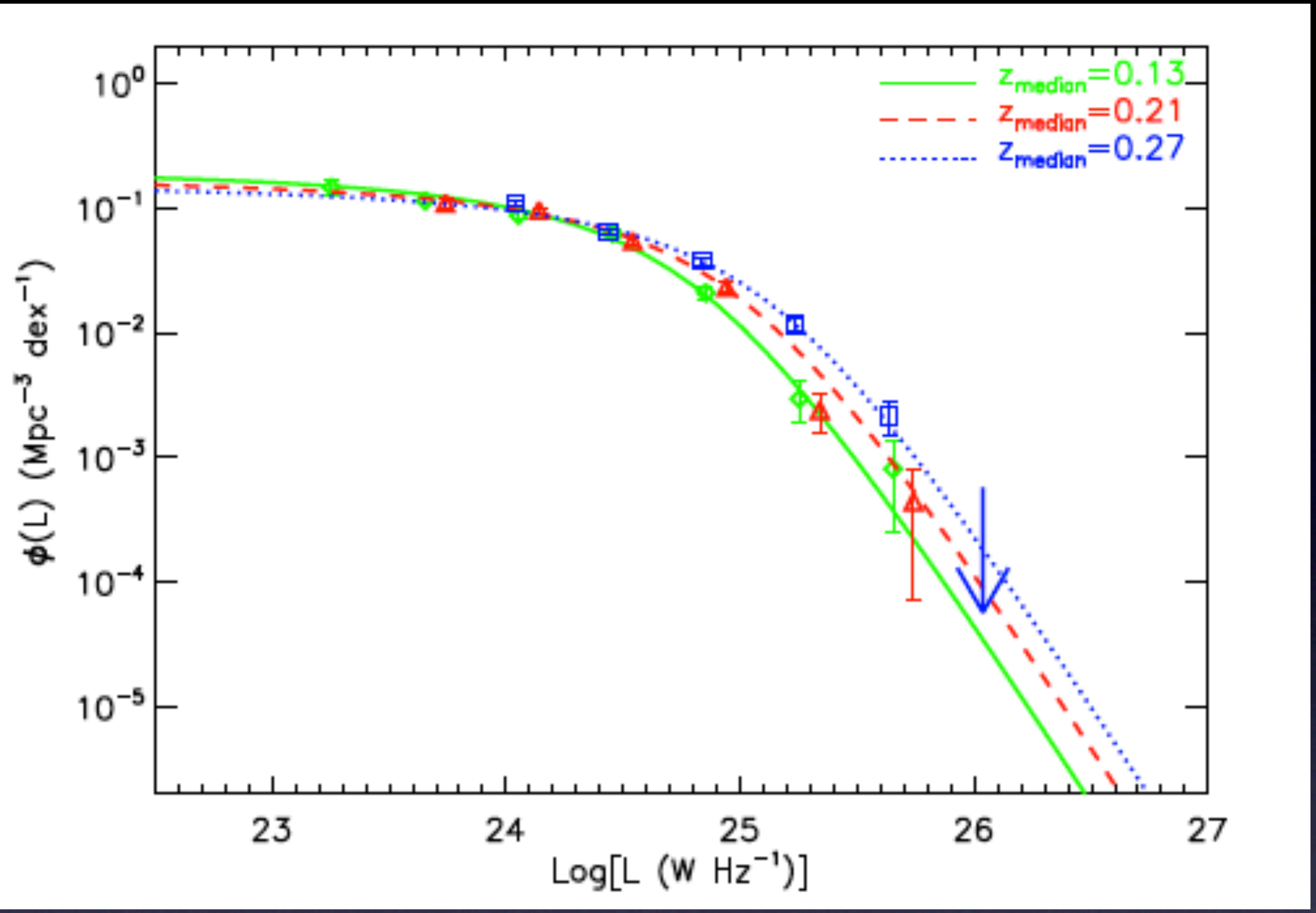

Cluster sample	Source catalog	Priors	y	b	x	w	α_ϕ	α_L	$\chi^2_{\rm red}$
maxBCG	FIRST		36.38±1.02	1.05±0.73	24.53±0.18	0.66±0.13	−2.46±1.58	6.20±1.76	1.07
maxBCG	FIRST	$\alpha_\phi = 0$	36.34±0.92	0.91±0.81	24.87±0.14	0.72±0.21	(0.0)	3.99±1.24	1.19
maxBCG	FIRST	$\alpha_L = 0$	36.74±0.89	1.01±0.55	25.11±0.11	0.71±0.19	1.03±1.14	(0.0)	2.25
X-ray	FIRST	(a)	36.19±0.19	(1.05)	(24.53)	(0.66)	0.76±1.86	8.12±2.67	0.94
X-ray	FIRST	(a); $\alpha_\phi = 0$	36.26±0.10	(1.05)	(24.53)	(0.66)	(0.0)	8.19±2.66	0.89
X-ray	FIRST	(a); $\alpha_L = 0$	35.89±0.18	(1.05)	(24.53)	(0.66)	9.40±1.85	(0.0)	10.48

Redshift evolution

X-ray sample

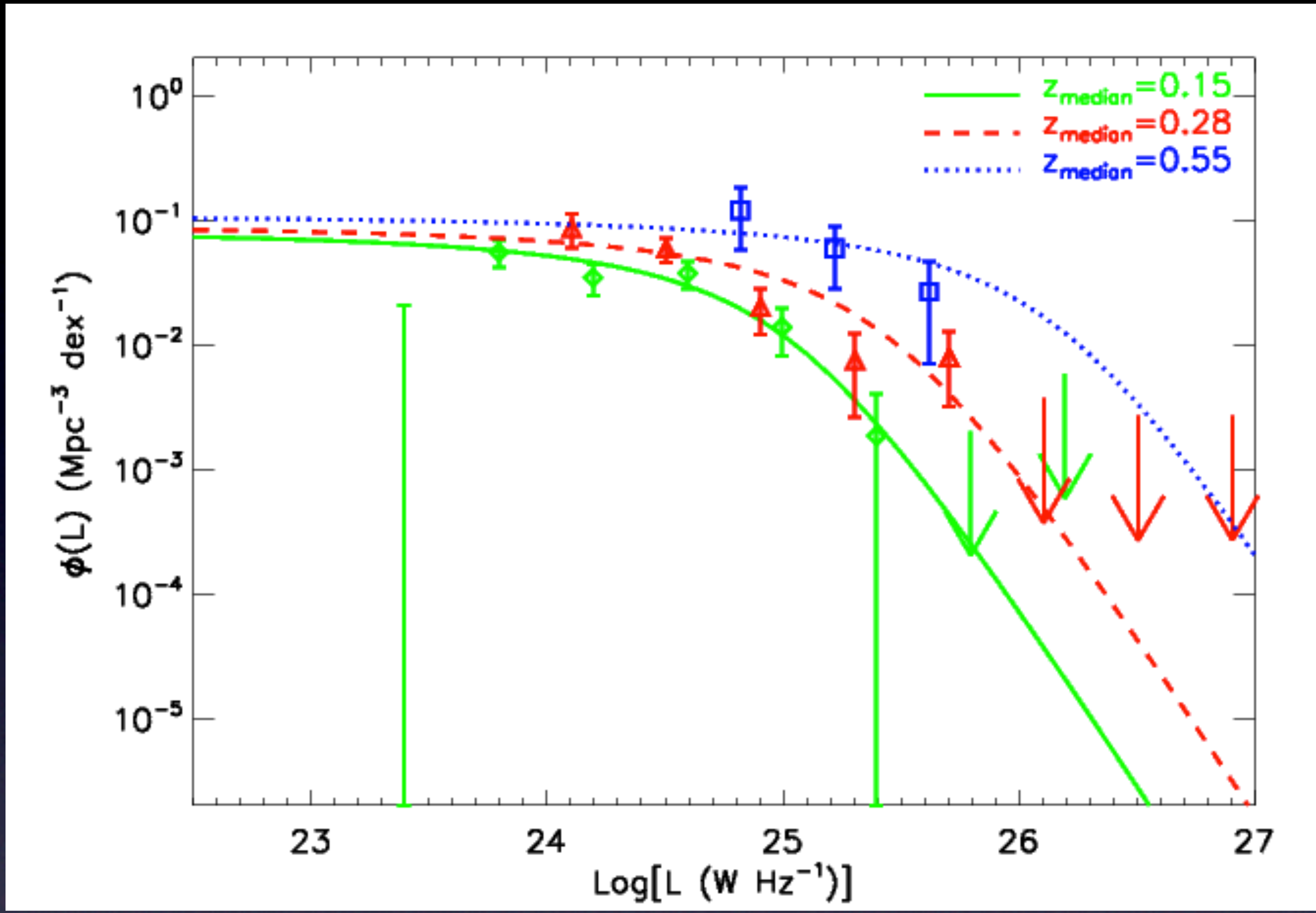

Cluster sample	Source catalog	Priors	y	b	x	w	α_ϕ	α_L	$\chi^2_{\rm red}$
maxBCG	FIRST		36.38±1.02	1.05±0.73	24.53±0.18	0.66±0.13	−2.46±1.58	6.20±1.76	1.07
maxBCG	FIRST	$\alpha_\phi = 0$	36.34±0.92	0.91±0.81	24.87±0.14	0.72±0.21	(0.0)	3.99±1.24	1.19
maxBCG	FIRST	$\alpha_L = 0$	36.74±0.89	1.01±0.55	25.11±0.11	0.71±0.19	1.03±1.14	(0.0)	2.25
X-ray	FIRST	(a)	36.19±0.19	(1.05)	(24.53)	(0.66)	0.76±1.86	8.12±2.67	0.94
X-ray	FIRST	(a); $\alpha_\phi = 0$	36.26±0.10	(1.05)	(24.53)	(0.66)	(0.0)	8.19±2.66	0.89
X-ray	FIRST	(a); $\alpha_L = 0$	35.89±0.18	(1.05)	(24.53)	(0.66)	9.40±1.85	(0.0)	10.48

Conclusions

We found that the luminosity of the most radio-luminous source within 50 kpc from the cluster center scales with cluster mass following a power law with slope 0.31 ± 0.12 in the maxBCG sample. This is consistent with the results of Lin & Mohr (2004) as well as with the results of our X-ray sample, although the latter is also consistent with no correlation.

We find the RLFs constructed from the optical and X-ray samples of galaxy clusters to be in approximate agreement. The RLF from the optical maxBCG sample is systematically lower at luminosities $L \gtrsim 3 \times 10^{25}$ W Hz^{-1}. This is likely a result of many more low-mass systems being present in the optical sample.

We provide the first evidence for a luminosity evolution of the volume-averaged RLF in clusters of galaxies. The maxBCG/FIRST data are consistent with a pure luminosity evolution, with power scaling with redshift as $L \sim (1+z)^{\alpha_L}$, where $\alpha_L = 6.20^{+1.76+0.19}_{-1.76-0.17}$ (statistical followed by systematic uncertainties). There is no indication of a mass dependence in the RLF from the present data. However, the results from the X-ray sample are consistent with the findings of LM07, that the most luminous radio sources reside in massive clusters. This is further corroborated by the fact that the RLF constructed from the maxBCG sample (which contains a smaller fraction of high-mass systems than both our X-ray sample and the sample of LM07) is steeper at higher luminosities.

Extra plots

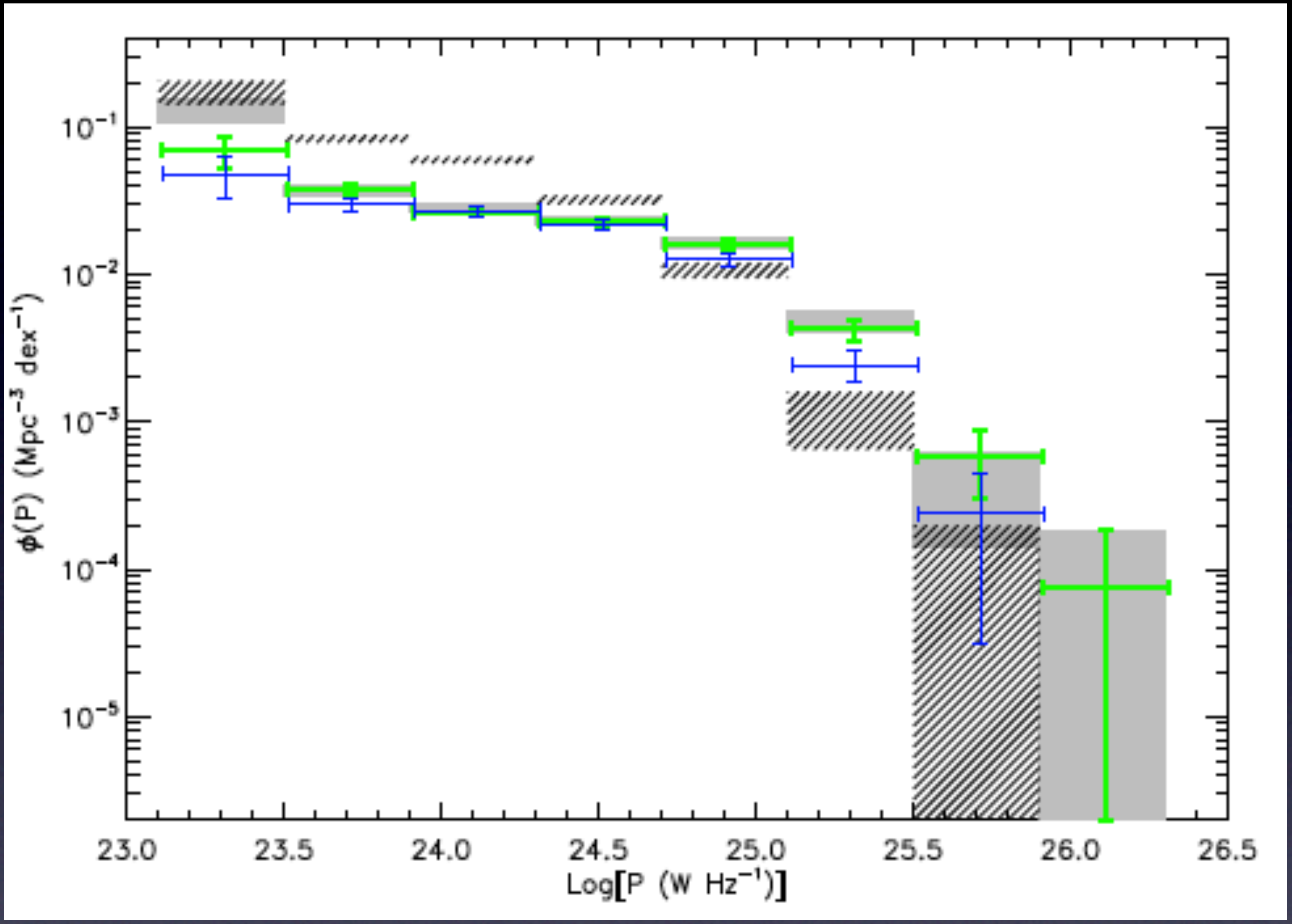

Comparison between NVSS and FIRST luminosity functions

Shaded regions: FIRST and NVSS uncorrected
Error bars: After degrading to a common resolution